

Kinetics and thermodynamics of sucrose crystallization from pure solution at different initial supersaturations

Issam A. Khaddour^{a,*}, Luís S.M. Bento^a, António M.A. Ferreira^{a,b}, Fernando A.N. Rocha^{a,*}

^a LEPE, Departamento de Engenharia Química, Faculdade de Engenharia, Universidade do Porto, Rua Dr. Roberto Frias, 4200-465 Porto, Portugal

^b IBB-Institute for Biotechnology and Bioengineering, Centre of Biological Engineering, Universidade do Minho, Campus de Gualtar, 4710-057 Braga, Portugal

ARTICLE INFO

Article history:

Received 5 January 2010

Accepted 7 April 2010

Available online 14 April 2010

Keywords:

Sucrose
Dehydration
Nucleation
Crystallization
Critical radius

ABSTRACT

Growth rates of sucrose crystallization from pure solutions of initial relative supersaturation levels between 0.094 and 0.181 were studied in agitated crystallizer at 313.13 K. Birth and spread model was applicable for the obtained growth rate data in this range of supersaturation and used to estimate the principal growth parameters. The estimated interfacial free energy varied inversely with supersaturation from 0.00842 to 0.00461 J/m², respectively. The obtained kinetic coefficient changed with the initial supersaturation from 9.45×10^{-5} to 2.79×10^{-7} m/s. The corresponding radius of the 2D (two dimensional) critical nucleus varied from 7.47×10^{-9} to 1.46×10^{-9} m. Predominance of surface integration or volume diffusion mechanism during the growth process was assessed using the calculated activation free energies of the 2D nucleation process. An acceptable confirmation of the calculated radius of the critical 2D nucleus was found using atomic force microscopy (AFM) technique. The calculated interfacial free energy between the saturated sucrose solution and the crystal surface was found to be 0.02325 J/m².

© 2010 Elsevier B.V. All rights reserved.

1. Introduction

Two limiting models were proposed to describe the growth of 2D nuclei on growing face of the crystal: the spreading velocity may be considered infinitely fast i.e. mononuclear model, or it is assumed to be negligibly small i.e. polynuclear model. However the more realistic model considers finite spreading rates i.e. birth and spread (B+S) model [1], as the concept of mononuclear involves discontinuity of the microscopic growth with respect to time, and discontinuity with respect to the surface layer will occur considering the polynuclear model. The key event in all the 2D nucleation models is the birth of critical nucleus [1–3].

$$\rho_c = v_m \gamma / kT \ln(1 + \sigma) \quad (1)$$

ρ_c (m) is the radius of the critical nucleus, γ (J/m²) is the interfacial free energy between the developing crystalline surface and the supersaturated solution in which it is located, v_m (m³) is the molecular volume and equals to 2.5542×10^{-28} for sucrose [4,5], k (JK⁻¹) is Boltzmann constant and equals to 1.3805×10^{-23} , T (K) is the temperature, and σ (dimensionless) is the relative supersaturation expressed in terms of activity of the supersaturated solution [1,2].

$$\sigma = \frac{a}{a^*} - 1 \quad (2)$$

where a and a^* are the activity of the solute in supersaturated and saturated solutions, respectively.

The detailed derivation of growth rate equation for the B+S model was mentioned by Ohara and Reid [1] and the final form is:

$$R = C_4 \sigma^{2/3} [\ln(1 + \sigma)]^{1/6} \exp \left[-C_2 / 3T^2 \ln(1 + \sigma) \right] \quad (3)$$

where

$$C_4 = 2h^{1/6} v_m^{5/6} (\omega / \pi)^{1/3} (n_1 D_s \beta \gamma_0 C_{SE} / X_s)^{2/3} \quad (4)$$

and

$$C_2 = \pi h \gamma^2 v_m / k^2 \quad (5)$$

R is the overall linear growth rate (m/s), h (m) is the single step height, ω (m/s) is the average speed of the surface adsorbed molecule. There is an argument concerning the estimation of this parameter as it can be calculated in two different ways, by $(\omega = \sqrt{8kT/M\pi})$ in terms of perfect gas approach, or by $(\omega = \frac{h}{\tau_s})$, where M is the molar mass of sucrose, f is the molecular frequency of vibration $f \approx \frac{kT}{h_p}$ and h_p is Planck constant 6.626×10^{-34} (J s), n_1 is the number of molecular monomers on the surface (m⁻²), D_s (m²/s) is the surface diffusion coefficient of the adsorbed molecule, β and γ_0 are the step and kink retardation factors, respectively, C_{SE} (m⁻²) is the equilibrium concentration of the solute on the surface, and X_s (m) is the mean diffusion distance of the solute on the surface during time τ_s (s), $X_s^2 \cong bD_s \tau_s$ (b is a constant that varies from 2, 4 and 6 for one-, two-, or

* Corresponding authors. Tel.: +351 225081678; fax: +351 225081449.
E-mail addresses: issamoali99@gmail.com (I.A. Khaddour), frocha@fe.up.pt (F.A.N. Rocha).

three-dimensional diffusion). The expected nucleation rates per unit area of the surface are given by the following equation,

$$I = \left(\frac{2\omega}{\pi} \right) n_1^2 \left[\frac{v_m \ln(1 + \sigma)}{h} \right]^{1/2} \exp(-\Delta G_c / kT) \quad (6)$$

ΔG_c (J/molecule) is the total Gibbs free energy change to form a nucleus of radius ρ_c ,

$$\Delta G_c = \pi h \gamma^2 v_m / kT \ln(1 + \sigma) \quad (7)$$

In spite of number of questionable assumptions and approximations used to derive Eq. (6), however it shows that the 2D-nucleation rates are very sensitive to temperature and supersaturation and, especially to the interfacial free energy γ . This is particularly true in growth from low temperature solutions where the range of the work temperatures is narrow, while the interfacial free energy strongly varies from face to face and with the solvent (or impurity) adsorption. Also, this model allows a growth order g to be greater than 2 which is not possible in other models [2].

$$R = K_f \sigma^g \quad (8)$$

K_f (m/s) is the linear growth rate coefficient.

This work reports experimental results on the growth rate kinetics and the interfacial free energies of sucrose crystallization as a function of the initial supersaturation. A trial to validate the calculated parameters from birth and spread model was made using atomic force microscopy technique.

2. Experimental section

2.1. Growth experiments

Growth rates of sucrose from pure solutions were measured from the determined crystallized sucrose mass with time during runs of 24 h (only one run was elapsed 72 h) using mass balance equations based on on-line refractometric readings for isothermal conditions at 313.15 K in 4 L jacketed and stirred stainless steel batch crystallizer. Stirring speed was set on 250 rpm. The temperature was controlled using water thermostatic bath with an accuracy of ± 0.01 °C.

Sucrose solutions were prepared from refined white sugar of purity of 99.95% (RAR refinery, Portugal). Sugar samples were dissolved until a determined concentration in ultra-pure water of resistivity $18.3 \mu\Omega \text{ cm}$ prepared through deionization process. The temperature of prepared solutions was elevated to 333.15 K for 20 h to ensure complete dissolution and homogeneity. Then, cooling down to the working temperature was done during 2 h. After the temperature became stable for more or less 1 h, an accurate mass of the seed crystals of 16.0000 ± 0.0010 g of mean size of $251.1 \mu\text{m}$ was introduced into the crystallizer. Crystals were allowed to grow during 24 h, and dissolved sucrose content was observed using on-line refractometer (Schmidt + Haensch iPR2).

2.2. Atomic force microscopy work

The same approach of growth experiments section was followed to achieve two runs with relatively high and low initial supersaturations, $\sigma_1 = 0.181$, and $\sigma_2 = 0.094$. For every run, two samples were taken at different time intervals: after 1.5 and 22.5 h, using peristaltic pump associated with vacuum filtration equipment. After the filtration, every sample was immersed in absolute ethanol with shaking for 5 min to clean the surface from the attached syrup. This process was repeated 5 times followed by final filtration of crystals. The last step was to dry 30 g, more or less, of the sugar using forced heated air at low flow rate, at 328.15 K for 15 min and 358.15 K for 5–10 min. Then,

an ex-situ examination of (100) faces by AFM was carried out at different locations.

AFM imaging of the crystal was conducted in contact mode using Multimode NanoScope IVa (Veeco, Santa Barbara, USA). Standard silicon nitride AFM tips (Veeco, Santa Barbara, USA) were used. Cantilevers with nominal force constants of 0.12 N/m were typically utilized, in order to minimize the force applied to the crystalline surface during scanning, and the set point voltage was continually adjusted to the lowest level for which tip-crystal contact was maintained. In AFM, the silicon nitride tips had an apex angle of 35° . Scanning frequency was typically 5 Hz with 512 lines per frame.

The accompanied software of this technique, specially the surface distance measurements and the cross section profile, allows the acquisition of principal information with high accuracy. Diameter of the surface nuclei was estimated from the surface distance using deflection images. Hundreds of images were processed and samples of the most representative ones are shown.

2.3. Size distribution of the crystals

Size distribution was determined by using COULTER LS230 laser sizer apparatus for the seed and final crystals. Absolute ethanol was used to clean and to fill the measuring cell of Coulter apparatus. Then, the sugar was added through the sample hole until 10% concentration. Through the output pattern of the scattered illuminating beam of laser one can find an indication on the occurrence of nucleation as well as conglomerates.

3. Calculations and treatment of the data

Growth rates were expressed in terms of overall mass deposition rate R_g , and calculated according to the following equation [2,6]

$$R_g = \frac{3\alpha_1^{2/3} \rho_s^{2/3} (M_f^{1/3} - M_i^{1/3})}{\beta_1 N_s^{1/3} \Delta t} \quad (9)$$

where R_g is the overall growth rate ($\text{kg/m}^2\text{s}$), α_1 and β_1 are the volume and surface shape factors and were taken to be 0.64 and 4.52, respectively, ρ_s is sucrose crystal density at the studied temperature, 1583.7 (kg/m^3), M_f and M_i (kg) are the deposited mass at the end and at the beginning of a certain time interval Δt , respectively, and N_s is the number of seed crystals. The two parameters α_1 and β_1 were calculated by Guimarães et al. [7] for more than 1000 cane refined sugar crystals from industrial crystallizer, for different fractions of sieve size, in a similar manner to those used by other authors [8,9].

The overall linear growth rate was evaluated from:

$$R = \frac{(M_f^{1/3} - M_i^{1/3})}{(\alpha_1 \rho_s N_s)^{1/3} \Delta t} \quad (10)$$

Activity coefficients for the sucrose pure supersaturated solutions at 313.15 K were estimated based on the works done by Ferreira [10] and Peres [11,12] using UNIQUAQ model.

To confirm that there was negligible effect of nucleation or conglomerates in the studied range of supersaturations the size distribution test was done for one run with an initial brix of sucrose concentration of 72.35 higher by ≈ 0.33 °Brix than the highest initial Brix concentration used in this work i.e. 72.023 ($\sigma = 0.181$). Fig. 1 shows fair accordance between size distribution curves for seeds and final crystals. The existence of crystals created by nucleation and crystal breakage, and conglomerates formed during filtration, washing and drying of the grown crystals, are evident in the figure. Nevertheless, the relative amounts of these crystals are not significant, not invalidating the hypothesis of no nucleation and agglomeration, and so not changing the obtained conclusions. When expressing the

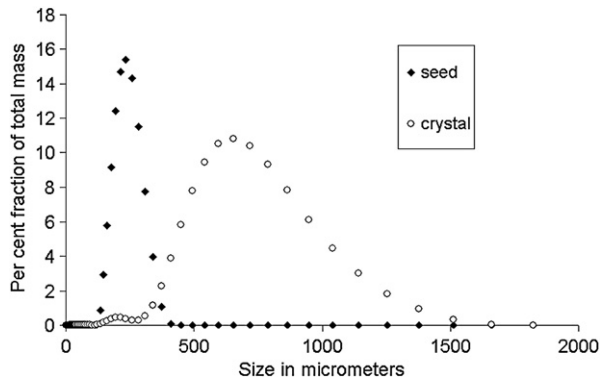


Fig. 1. Final crystal and seed size distributions for a growth experiment at the initial concentration of 72.35% of sucrose in solution.

degree of supersaturation by $S = \frac{c}{c^*}$, where c is the concentration of sucrose in solution in grams per 100 g of water, and c^* is the concentration of sucrose in grams per 100 g of water in a saturated solution at the same temperature, a metastable zone of width of $S=1-1.2$ was estimated in the case of non-seeded solution, i.e. primary homogenous nucleation starts beyond $S=1.2$ [13,14]. In this work the working zone varied from 1.05 to 1.1. Data for seeded solutions are not available, however, it was pointed out [15] that a narrower metastable zone would be expected in this case.

Determination of the characteristic length of the crystal L_t at certain time t was obtained from the corresponding crystallized mass M_t at the time t by $L_t = \sqrt[3]{\frac{M_t}{\alpha_1 \rho_s}}$.

Application of the B+S model was done by graphing $\left(\ln\left(\frac{R}{\sigma^{2/3}[\ln(1+\sigma)]^{1/6}}\right)\right)$ versus $\left(\frac{1}{3T^2 \ln(1+\sigma)}\right)$. The interfacial free energy between the supersaturated solution and the crystal surface was estimated using Eq. (5). For that, C_2 values were determined from the slope of the obtained equations of the fitting by linear regression type. The values of the kinetic coefficient C_4 for the different runs were determined from the corresponding intercept.

It is necessary to point out that the obtained kinetic parameters (C_4), the interfacial free energy, and the activation free energy ΔG_c required to form one 2D nucleus as well as the radius of the 2D nucleus represent rough averaged values of these parameters over all the growing faces of the crystal as they are estimated using the overall growth rate and not from face-by-face growth rate studies.

Rough estimation of the required number of sucrose molecules to form one 2D critical nucleus at certain supersaturation level was calculated using the corresponding critical radius by the equation: $N = \frac{\pi \rho^2}{v_m^{2/3}}$.

Mersmann [2,15,16] proposed an equation to estimate the interfacial free energy at saturation conditions for more than 50 systems (the concentration profile was replaced by the activity profile). This equation was used to determine the interfacial free energy between the saturated sucrose solution and the sucrose crystal at 313.15 K (the concentration profile was replaced by activity profile).

$$\gamma = \frac{0.414kT}{d_m^2} \ln\left(\frac{a_1}{a^*}\right) \quad (11)$$

$d_m \approx v_m^{1/3}$ is the molecular diameter of sucrose, and a_1, a^* are the solute activity in solid phase and for the liquid phase at saturation, respectively. The activity of solid phase was considered to be equal to the concentration of sucrose in its solid phase in kmol/m³, i.e. 4.6266, which implies that the activity coefficient was considered to be equal to one, meaning that the structure of the crystal is perfect and no water is included inside the crystal. This is reasonable to suppose as

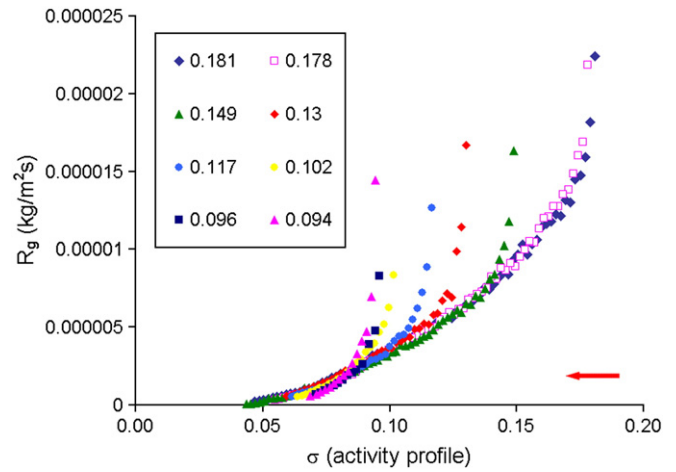


Fig. 2. Progression of the estimated growth rates R_g as a function of the relative supersaturation σ over the duration of the conducted runs at different initial supersaturations. The arrow indicates the direction of the process with time.

the normal value of moisture content in the refined sugar is lower than 0.05% [14]. Deficiencies associated with Mersmann equation could be related to the unknown steric effects or to the different interaction forces of the sucrose and the water or both. Also solvation of water molecules with sucrose molecules and dissociation of molecules may play a role [16–18]. In fact all these effects could be reduced considerably as the concentration was expressed in terms of activity coefficients of sucrose, keeping in mind that Mersmann appreciated the role of activity coefficients to reduce the found errors of his formula.

4. Results and discussion

4.1. Kinetics and thermodynamics

The calculated R_g and R_g/L_t are represented versus σ in Figs. 2 and 3, respectively. Application of birth and spread model is shown in Fig. 4 and the obtained results are presented in Table 1. The effect of growth rate history [6,19–22] is clearly shown in both Figs. 2 and 3, when all runs are compared with the run of highest initial supersaturation. Different values of growth rate were obtained for the same supersaturation. R_g was normalised by L_t to confirm the effect of growth rate history. Overlapping is shown in the last part of the curves (Fig. 3), which indicates the vanishing of the effect growth rate history phenomenon.

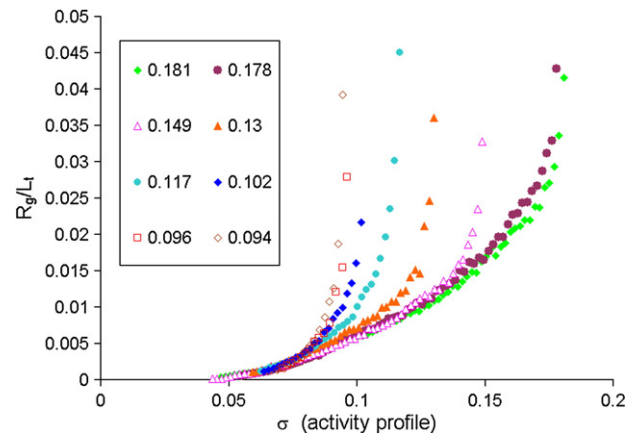


Fig. 3. Evolution of the ratio R_g/L_t as a function of the relative supersaturation σ over the growth period.

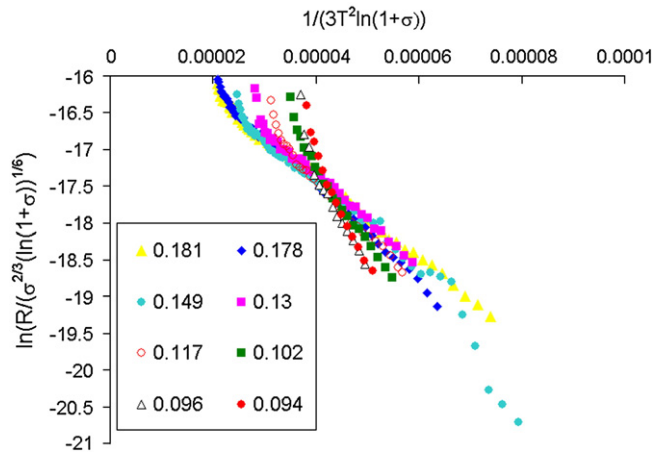


Fig. 4. Application of the B + S model. The goodness of fitting by linear regression R^2 varied from 0.92 to 0.99.

A noticeable steep reduction of the growth rate was recorded for a short range of σ at the beginning of every run, Fig. 2. For example, the run of initial $\sigma = 0.149$ continued for 72 h and 40 min. During the first 24 h the crystallized mass was 92.68% of the total crystallized mass, while in the remaining time only 7.32% was formed. It was also observed that around 30% of the total crystallized mass accumulated during the first 3 h. The relatively high growth rates in the first period of the growth process, specially in the case of high supersaturation group (0.181, 0.178, 0.149, and 0.13), are accounted to the predominance of sucrose–sucrose interactions in solutions of concentration higher than 2/3 of saturation concentration which leads to form swarms of sucrose clusters in the solution [18,23,24]. When the seeds are introduced into the solution these clusters deposit on the surface and work as sub-critical nuclei (protonuclei) for the 2D critical nuclei.

In the case of lower initial supersaturation group (0.094, 0.096, 0.102, and 0.117) the existence of the surface deposited clusters is expected, but, with lesser extent. However, the role of the sucrose surface diffused monomers is expected to be of major importance. The repeatedly reported increase of the role of surface diffusion at lower initial supersaturation values [25,26] is expected to augment the effect of growth rate history by increasing the kinetic coefficient values. Bennema [27] and Gilmer [25] reported dramatic increase in the growth rate when the surface diffusion plays the essential role than the volume diffusion process in which the integration into the available kinks on the steps is the rate determining step. For sucrose case, the dehydration process is necessary to incorporate the sucrose molecules into the available kinks. Bernal and Van Hook [28] demonstrated the electrorestricive hydration of sucrose which means that hydrogen bonding between water and sucrose is as strong as that found for strong electrolytes. One can conclude that the

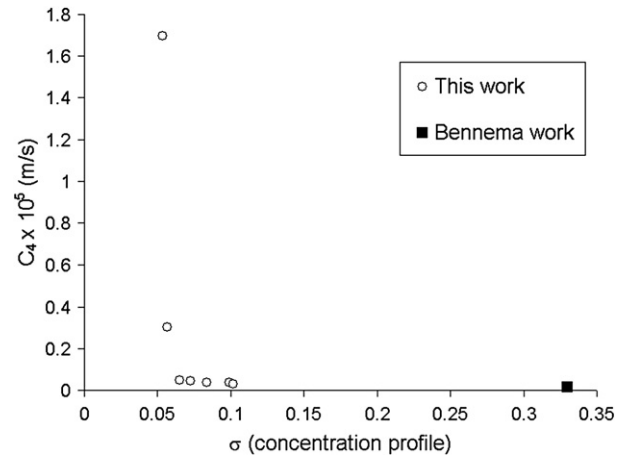


Fig. 5. Variation of the estimated kinetic coefficient (C_4), from birth and spread model, with initial relative supersaturation (σ) in concentration profile (the value for $\sigma = 0.094$ is not shown due to a scale question).

dehydration of the bonded water molecules during the integration step slows the growth process [18,24,29] i.e. lower kinetic coefficients are expected which is the case for higher initial supersaturation group in this work.

The average crystal size for the run of initial $\sigma = 0.094$ was 3.88×10^{-4} m, and 5.98×10^{-4} m for $\sigma = 0.181$. The increase of surface diffusion for crystals of smaller sizes is also in accordance with Valčić's [21] proposition. He used small crystals to have surface diffusion control throughout his experiments instead of using very high agitation speed.

The obtained growth rate curves show a practical stoppage of the growth process at $\sigma \approx 0.04$ (activity profile), which indicates the significance of the clustering of sucrose molecules and the surface nucleation throughout the process under the studied conditions, and particularly in the initial period of growth. A comparison of these curves with the nucleation and growth ones reported by VanHook [30], Mathlouthi and Genotelle [18], Dunning [31], Sönhel and Garside [32] and Aquilano et al. [33] offers almost no doubt regarding this conclusion.

Bennema [34] found, using Smythe's [35,36] data for sucrose at 313.75 K and relative supersaturation of 0.33 (concentration profile), a kinetic coefficient C_4 equal to 1.5×10^{-7} m/s. Taking into account the 0.5 °C temperature difference, his estimation is in a very good agreement with the trend of the kinetic coefficients obtained in this work, Fig. 5.

There is no available data on the estimation of the radius or the number of sucrose molecules to form one 2D critical nucleus. However, VanHook [30] predicted a radius of about 20 Å and from 80 to 100 molecules to form one 3D spherical shape critical nucleus from

Table 1

Kinetic coefficients, interfacial free energies and the corresponding characteristic parameters of 2D nuclei at the beginning ($\rho_{c(\text{beg.})}$, $N_{(\text{beg.})}$, $\Delta G_{\text{beg.}}$) and at the end ($\rho_{c(\text{end.})}$, $N_{(\text{end.})}$, $\Delta G_{\text{end.}}$) of the runs obtained by the application of the B + S model.

Relative supersaturation				$C_4 \times 10^7$ m/s	$\gamma \times 10^2$ J/m ²	$\rho_{c(\text{beg.})} \times 10^9$ M	$\rho_{c(\text{end.})} \times 10^9$ M	$N_{\text{beg.}}$	N_{end}	$\Delta G_{\text{beg.}} \times 10^{20}$ J/molecule	$\Delta G_{\text{end}} \times 10^{20}$ J/molecule
At beginning		At the end									
Activity profile	Concent. profile	Activity profile	Concent. profile								
0.181	0.102	0.047	0.026	2.79	0.461	1.64	5.93	21	275	1.51	5.45
0.178	0.099	0.055	0.030	3.63	0.497	1.79	5.49	25	235	1.78	5.44
0.149	0.083	0.044	0.024	3.81	0.501	2.13	6.91	35	373	2.13	6.9
0.13	0.073	0.060	0.033	4.46	0.502	2.43	5.13	46	205	2.42	5.13
0.117	0.065	0.062	0.034	8.03	0.557	2.98	5.51	69	237	3.31	6.12
0.102	0.057	0.064	0.035	30.2	0.646	3.95	6.17	121	297	5.08	7.95
0.096	0.054	0.071	0.039	170	0.762	4.90	6.56	187	336	7.44	9.96
0.094	0.053	0.069	0.038	945	0.842	5.50	7.47	236	435	9.23	12.5

concentrated sucrose solutions by primary nucleation process. This estimation is of close magnitude to the obtained range in this work, since 21 to 435 molecules (corresponding to critical radii of 1.64 to 7.47 nm, Table 1) were expected to form one nucleus from the applied range of supersaturations and during the entire time of the runs. In general, one could expect the 2D nucleus to have much smaller forming molecules than the 3D nucleus. But, the thermodynamic and the kinetic effects together should be kept in mind when a decrease of the supersaturation level is made. In fact, higher coverage of the surface by the growth units is expected when the growth process occurs with surface diffusion than without. For that, the surface diffusion can induce an overestimate of the required number of molecules to form one 2D critical nucleus in the case of lower initial supersaturation group.

Pantaraks et al. [20] pointed out that the diameter of the observed nuclei on the surface was of the size 1–10 μm , which represents in minimum 66 times of B + S estimations. However, the used ex-situ examination of the surface by AFM cannot predict the elapsed time since a certain found body on the surface was born.

The interfacial free energy for sucrose at $T = 313.15\text{ K}$ was calculated using Eq. (11), and the value of 0.02325 J/m^2 was obtained. The benefit of this calculation is to predict approximately the maximum value of γ (averaged over all faces of the crystal) which can be expected between the crystal and the solution, before complete stoppage of the crystallization process at the concerned temperature.

The interfacial free energies from crystallization experiments and at saturation are plotted in Fig. 6. The higher interfacial free energy obtained at lower initial supersaturations (Table 1) supports that the kinetic factors prevail over the free energy factors at these conditions, and confirm, from other side, the essential role of surface diffusion step.

Pantaraks et al. [20] mentioned 0.0047 J/m^2 as interfacial free energy for sucrose which is very close to the predicted range of this work. Primary nucleation of concentrated sucrose syrups was investigated by Dunning and Shipman [37], VanHook [30], VanHook and Bruno [38] and values of around 0.005 J/m^2 for the interfacial free energies were calculated.

4.1.1. Activation free energy of growth

Mullin [2] pointed out that the activation free energies for volume diffusion are usually $\approx 10\text{--}20\text{ kJ/mol}$ and for surface integration $\approx 40\text{--}60\text{ kJ/mol}$. Smythe [35] stated that the activation free energy for the volume diffusion in sucrose crystal growth is between 29.3 and 37.7 kJ/mol. On the other side Bennema [34] determined that the activation free energy for the surface integration of sucrose is between 65.7 and 69.9 kJ/mol. Schleiphake and Austemyer [39] estimated an activation free energy equal to 85.8 kJ/mol for the surface integration of sucrose.

VanHook [40] reported that the activation free energy at 40°C and $\sigma = 0.05$ (concentration profile) is $\approx 49\text{ kJ/mol}$. The calculated activation free energies (expressed in kJ/mol) at the beginning and

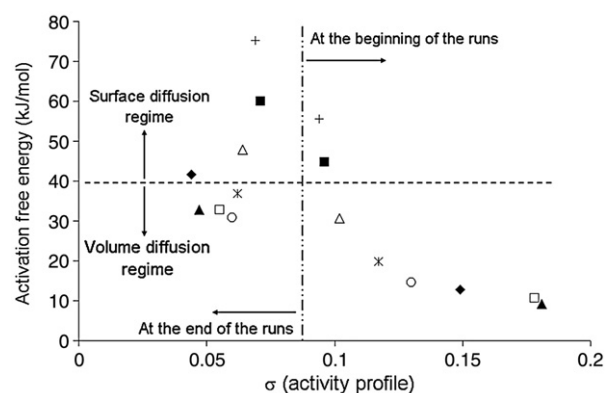


Fig. 7. Activation free energies at the beginning and at the end of the growth period plotted versus the corresponding initial and final values of supersaturation (activity profile) for every run.

at the end of the runs from the data given in Table 1, were plotted against σ (activity profile). The estimated activation free energies (9.1–75.3 kJ/mol) are a function of the initial supersaturation and duration of the run. These values are in a very good agreement with the literature values. The obtained trend of the activation free energies of growth versus σ in Fig. 7 is similar to that shown by VanHook [40] for the activation free energies versus temperature. Classification of the made runs between the surface diffusion regime and the volume diffusion one is presented based on the calculated free energies of activation (Fig. 7); this was made by considering 40 kJ/mol as separation line between these two regimes. Again one should state that the obtained activation free energies are averaged over all the available faces for growth of sucrose crystal during the experiments, since different growth mechanisms can occur at once on different faces [21]. For example Aquilano et al. [33] reported from face-by-face study on growth of sucrose crystal from pure aqueous solution in the range of $30\text{--}45^\circ\text{C}$ that the (101) and (110) faces grow by surface diffusion (the corresponding ΔG being 96 kJ/mol), while the (110) face is ruled mainly by volume diffusion (the corresponding ΔG being

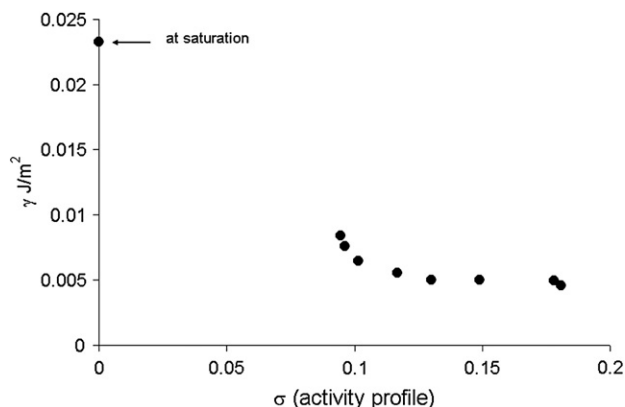


Fig. 6. Calculated interfacial energies, γ , at saturation and from growth experiments as a function of the initial relative supersaturation, σ (activity profile.)

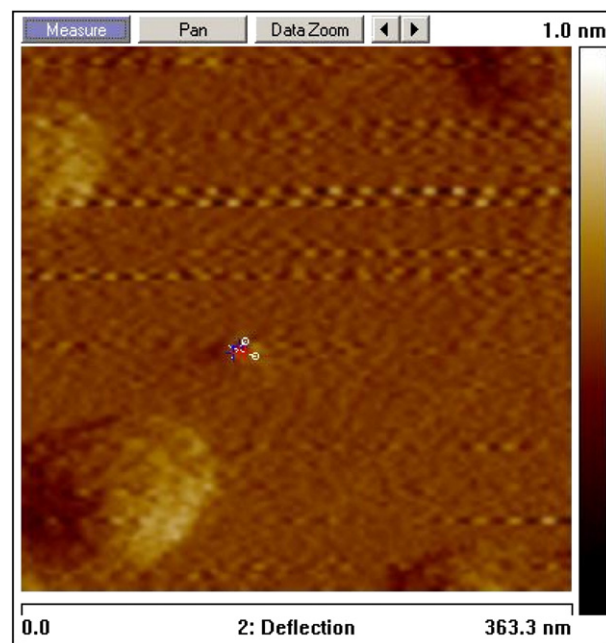


Fig. 8. Nucleus, 16 nm diameter, after 1.5 h of growth for initial supersaturation $\sigma = 0.181$, observed on face (100). The crossed red and blue marked lines measure the diameter of this nucleus.

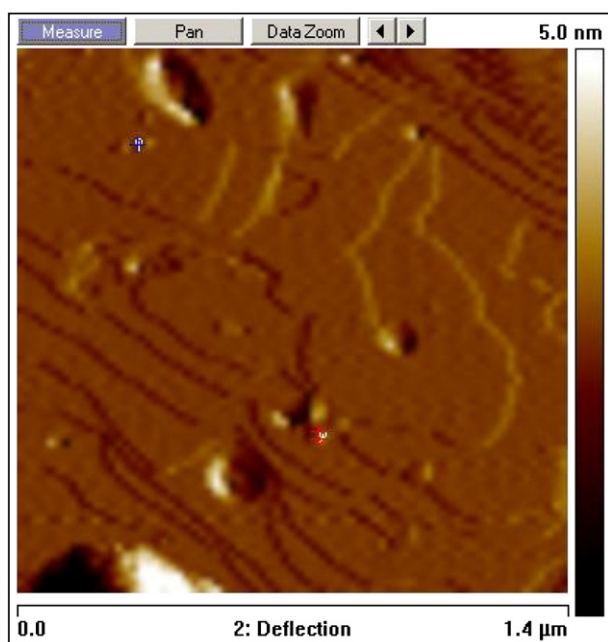


Fig. 9. Nuclei, 25 nm diameter, after 1.5 h of growth for initial supersaturation $\sigma = 0.094$, observed on face (100). The examined nuclei are blue and red marked.

42 kJ/mol). It is also noted that after prolonged time of growth (more than 72 h of growth) the run of $\sigma = 0.149$ starts to grow by surface diffusion mechanism. Fig. 7 shows also the incremental role of surface diffusion mechanism for the low initial supersaturation group (0.117, 0.102, 0.096, and 0.094). The increased role of volume diffusion for crystals with larger sizes is also noted (corresponds to higher initial supersaturations group) and this also is in accordance with Valčić's proposition [21].

4.2. Evaluation of the radius of the 2D critical nucleus by AFM

Face (100) was selected to conduct a study to confirm the calculated radius of the 2D nucleus, Table 1. For that, the radius of the found bodies on the crystal surface was estimated using atomic force microscopy technique. The attention was drawn to the smallest nucleus that could be found on the surface. The smallest observed body on the surface was more ellipsoidal than circular, with a mean diameter of ≈ 16 nm after 1.5 h of growth for initial supersaturation $\sigma = 0.181$, Fig. 8. Also a nucleus with a diameter of ≈ 18 nm was found after 22.5 h. As an acceptable approximation these values are close to the calculated range of critical diameters of nuclei ≈ 3.5 and 12.5 nm after 1.5 and 22.3 h, respectively. In fact, one cannot consider these found nuclei on the surface to represent exactly the real time situation. For example, the elapsed time since the formation of these nuclei is unknown. For initial supersaturation $\sigma = 0.094$, the diameter of the smallest observed nucleus was ≈ 25 nm after 1.5 h of growth, while the calculated one was ≈ 12 nm, Fig. 9. The difference between the calculated and the observed diameter of the nuclei can be attributed to the variation of surface concentration of the sucrose molecules [41], as well as to the way of selecting the areas of measurement. Also it can be related to the difference between the averaged interfacial free energy over all the crystal faces as found from the application of the B + S model and the exact value of interfacial free energy γ_{100} (or more accurately the edge free energy of the 2D nucleus periphery) of the face (100) which requires a separate growth study for this face. The large number of the observed nuclei on the crystal surface in both studied surfaces, especially during the first period of growth (after 1.5 h), confirms the role of the surface nucleation during the process (the related figures are

not shown). Vekilov [42] pointed out the significant role of 2D nucleation when the bulk relative supersaturation (concentration profile) is ≤ 0.1 which is the case of this study, Table 1.

In spite of many precautions that have to be taken when measuring the radius by this approach and the found difficulties of the method, however it represents an attempt to size those surface bodies and to understand more about their geometry.

5. Conclusions

1. Applicability of the B + S model to estimate the principal parameters of the growth process is shown, and it is in accordance with Lewis's conclusion on modelling the growth rate of macroscopic crystals [43].
2. Incorporation of sucrose molecules into the available kinks on the crystal surface is accompanied with dehydration step. This step is of higher importance at higher initial supersaturation levels than at lower supersaturation levels.
3. Clustering of sucrose molecules (swarms) at relatively high initial supersaturations, and surface diffusion at low initial supersaturations, induce fast growth rates at the initial period of the growth process.
4. Activation free energy of the growth process decreases with increase of initial supersaturation. This effect is similar to that shown by the increase of temperature [40].
5. Precise and careful measurement of the diameter of 2D nuclei, using AFM technique, provides a tool to confirm and correct the calculated interfacial free energy values. This measurement is of great importance for the growth process at relatively low initial supersaturation.

Acknowledgements

The funding from Syrian Ministry of Higher Education and FEUP (Portugal) is highly appreciated.

We would also like to express our sincere gratitude to Mr. Rui Rocha for doing the AFM analyses and related discussion.

References

- [1] M. Ohara, R.C. Reid, Modelling Crystal Growth Rates from Solution, Prentice-Hall Inc., New Jersey, 1973.
- [2] J.W. Mullin, Crystallization, Butterworth-Heinemann, Oxford, 2001.
- [3] K. Sangwal, Prog. Crystal Growth and Charact. 36 (1998) 163.
- [4] A.G. Rasmussen, PhD thesis, Technical University of Denmark, 2001.
- [5] Cambridge Data Base. Reference code: 00-024-1977.
- [6] A. Ferreira, N. Faria, F. Rocha, J. Cryst. Growth. 310 (2008) 442.
- [7] L. Guimarães, S. Sa, L.S.M. Bento, F. Rocha, Int. Sugar J. 97 (1995) 199.
- [8] Z. Bubnik, P. Kadlec, Zuckerind. 117 (1992) 345.
- [9] A. VanHook, Ind. Sacc. Ital. 55 (1962) 217.
- [10] A. Ferreira, PhD Thesis, Universidade Do Porto, 2008.
- [11] A.M. Peres, E.A. Macedo, Fluid Phase Equilibria. 123 (1996) 71.
- [12] A.M. Peres, PhD Thesis, Universidade Do Porto, 1998.
- [13] P. Honig, Principles of Sugar Technology, Vol. II, Elsevier, Amsterdam, 1959.
- [14] J.C.P. Chen, C.C. Chou, Cane Sugar Handbook, 12th ed. Wiley & Sons, New York, 1993.
- [15] A. Mersmann, Crystallisation Technology Handbook, Marcel Dekker Inc, New York, 1995.
- [16] A. Mersmann, J. Cryst. Growth 102 (1990) 841.
- [17] A. VanHook, Int. Soc. Sugar Cane Tech. 3 (1977) 2613.
- [18] M. Mathlouthi, J. Genotelle, Carbohydr. Polym. 37 (1998) 335.
- [19] P. Pantarakas, A.E. Flood, Cryst. Growth Des. 5 (2005) 365.
- [20] P. Pantarakas, M. Matsuoka, A.E. Flood, Cryst. Growth Des. 7 (2007) 2635.
- [21] A.V. Valčić, J. Cryst. Growth 30 (1975) 129.
- [22] P.M. Martins, F. Rocha, Cryst. Res. Technol. 43 (2008) 1258.
- [23] N. Tikhomiroff, F. Heitz, Utilisation du microcalorimètre Calvet pour la détermination des chaleurs et des vitesses de cristallisation. In *Compte-rendus du congrès de calorimétrie*, Marseille, (1965) 341–355.
- [24] J. Genotelle, M. Mathlouthi, B. Rogé, M. Starzak, M. In Euro Food's Water: 5th International Workshop on Water in Food, <http://www.efw2008.de/>, Nürtingen, 2008.
- [25] G.H. Gilmer, Faraday Symp. Chem. Soc. 12 (1977) 59.
- [26] W.K. Burton, N. Cabrera, Disc. Faraday Soc. 5 (1949) 40.
- [27] P. Bennema, J. Cryst. Growth 1 (1967) 278.

- [28] P.J. Bernal, W.A. Van Hook, J. Chem. Thermodyn. 18 (1986) 955.
- [29] A. VanHook, Int. Soc. Sugar Cane Tech. 3 (1977) 2613.
- [30] A. VanHook, Crystallization: Theory and Practice, Reinhold, New York, 1961.
- [31] W.J. Dunning, Discuss. Faraday Soc 5 (1949) 79.
- [32] B.M. Söhnel, J. Garside, Precipitation: Basic Principle and Industrial Applications, Butterworth-Heinemann, Oxford, 1992.
- [33] D. Aquilano, M. Rubbo, G. Mantovani, G. Vaccari, G. Sgualdino, ACS Symp. Series 438, Ch.6, 1990, p. 72.
- [34] P.J. Bennema, Cryst. Growth 3 (4) (1968) 331.
- [35] B.M. Smythe, Australian J. Chem. 20 (1967) 1087.
- [36] B.M. Smythe, Australian J. Chem 20 (1967) 1097.
- [37] W.J. Dunning, A. Shipman, J. Proc. Agric. Ind, X Int. Cong. (1954) 1 Madrid.
- [38] A. VanHook, A. Bruno, J. Disc. Faraday Soc. 5 (1949) 122.
- [39] D. Schliephake, K. Austmyer, Zucker. 29 (1976) 293.
- [40] A. VanHook, Ind. Eng. Chem. 37 (1945) 782.
- [41] K. Tsukamoto, in: I. Sungawa (Ed.), Morphology and Growth Unit of Crystals, Terra Scientific Pub. Co, Tokyo, 1989, p. 451.
- [42] P.G. Vekilov, Cryst. Growth Des. 7 (2007) 2796.
- [43] B. Lewis, J. Cryst. Growth 21 (1974) 29.